Response to review comments on "A generalised Gaussian wake model based on extended actuator disc theory" by Fei et al. (wes-2026-76)

We thank the referees for these helpful comments. We agree that the original manuscript did not sufficiently clarify the assumptions behind the proposed model. In response, we have revised the manuscript accordingly and summarise the main changes below.

Response to referee 1

- Response to major concern 1:

  - Definition of the near-far wake location

    We thank the referee for pointing out the inconsistency in the definition. We admit the concepts could have been explained more clearly. In our revised manuscript, we clarify that the Gaussian wake profile is not used as a definition of the transition to far wake. Rather, the start of the far wake is defined as the inflection point of wake centreline velocity α. However, since the dominant driving forces of the variation of α are $\partial\hat{p}/\partial\hat{x}$ and $\mathcal{R}$ as shown in Section 3.1, we take the start of the far wake at the location where $\mathcal{R} - \partial\hat{p}/\partial\hat{x}$ reaches its maximum. Once $\mathcal{R} - \partial\hat{p}/\partial\hat{x}$ reaches its maximum, the velocity profile is assumed to be fully developed and reaches a self-similar state. In this case, as is adopted by many studies, we take the self-similar velocity profile to be Gaussian.

    The evolution of the wake profile is directly linked to the streamwise variation of the Reynolds-stress divergence, $\mathcal{R}$. Two distinct regimes can be identified.

    In the first regime, the wake profile evolves from the initial state, which is usually taken to be top-hat, to the self-similar state, which is usually taken to be Gaussian. During this stage, the profile evolution itself contributes to an increase in $\mathcal{R}$. In the second regime, once the profile has become self-similar, the subsequent evolution of $\mathcal{R}$ is governed primarily by changes in the maximum velocity deficit, C, and wake width, σ. Importantly, here $\mathcal{R}$ decreases with the reduction of C and the increase of σ. Thus, the wake profile tends to be self-similar (Gaussian) in the region where $\mathcal{R}$ decreases.

    Since $\partial\hat{p}/\partial\hat{x}$ continuously decreases downstream of the turbine towards the far wake, the maximum $\mathcal{R} - \partial\hat{p}/\partial\hat{x}$ occurs downstream of the maximum $\mathcal{R}$. This means that the wake profile tends to be already self-similar where $\mathcal{R} - \partial\hat{p}/\partial\hat{x}$ is maximum.

    It should be noted that a limiting case may exist under very low inflow turbulence in which the wake profile has not fully developed when $\mathcal{R}$ begins to decrease. However, in such a situation, the profile must already be close to the fully developed state. Otherwise, the continuing profile-shape evolution would still provide a considerable positive contribution to $\mathcal{R}$, preventing the observed net decrease.

    This explanation is included from line 220 to 226 in the revised manuscript.

  - Regarding the flatness in Fig. 12

    Regarding the referee's observation of the low-turbulence case in Fig. 12, we note that the velocity profile shown in that figure is extracted at the location satisfying $\mathcal{R} = \int_{-\infty}^{\hat{x}} \mathcal{R}(\xi)d\xi$ rather than at the location where $\mathcal{R} - \partial\hat{p}/\partial\hat{x}$ is maximum. As discussed in the original manuscript from line 211 to line 213, these two locations do not coincide exactly, particularly under low-turbulence conditions. The latter is our proposed proxy of the start of the far wake, whereas the former is another (practical) approximation. The discrepancy observed in the low-turbulence case, therefore, reflects the limitation of the approximation rather than a problem in the proposed definition of the start of the far wake. We now clarify this distinction explicitly in lines 485-486 in the revised manuscript.

  - Regarding the inflection point

    With regard to the referee's minor comment concerning the terminology of the inflection point, we include $\partial^2\hat{u}/\partial\hat{x}^2$ in Fig.4 in the manuscript.

  - Why the maximum $\mathcal{R} - \partial\hat{p}/\partial\hat{x}$ and the point where $\mathcal{R} = \int_{-\infty}^{\hat{x}} \mathcal{R}d\xi$ are so close

    As for the physical interpretation of why the point where $\mathcal{R} - \partial\hat{p}/\partial\hat{x}$ is maximum and the point where $\mathcal{R} = \int_{-\infty}^{\hat{x}} \mathcal{R}d\xi$ are close, we emphasize that the hypothesis is not derived from any specific turbulence closure. Rather, it originates from the physical reasoning that they both tend to occur when $\mathcal{R}$ is large compared to $\partial\hat{p}/\partial\hat{x}$. Thus, we expect that the same hypothesis can be made for different turbulence models, but the agreement may vary. We include further clarification and analysis on the physical meaning behind this hypothesis in Section 3.2 from line 232 to 233 in the revised manuscript.

- Major comment 2: Is the quantity $\mathcal{R}$ continuous across the turbine disc

  Physically, the centreline $\mathcal{R}$ is continuous across the disc, as it is the divergence of the Reynolds shear stresses. For the actuator disc model considered, the mean velocity field is continuous across the disc, so $\mathcal{R}$ is also expected to be continuous.

  In the simulation, the value of $\mathcal{R}$ seems to change quite quickly because the velocity profile along the spanwise direction changes quickly. The components of $\mathcal{R}$ from the simulation are displayed in the figure below. From this figure, we can see that $\mathcal{R}$ changes quickly across the disc because $\partial^2\hat{U}/\partial\hat{y}^2$ and $\partial^2\hat{U}/\partial\hat{z}^2$ change quickly across the disc. Nevertheless, these changes are finite and correspond to changes in the wake profile. Thus, $\mathcal{R}$ is continuous across the disc. The clarification is added in Section 3.1 from line 187 to 188 in the revised manuscript.

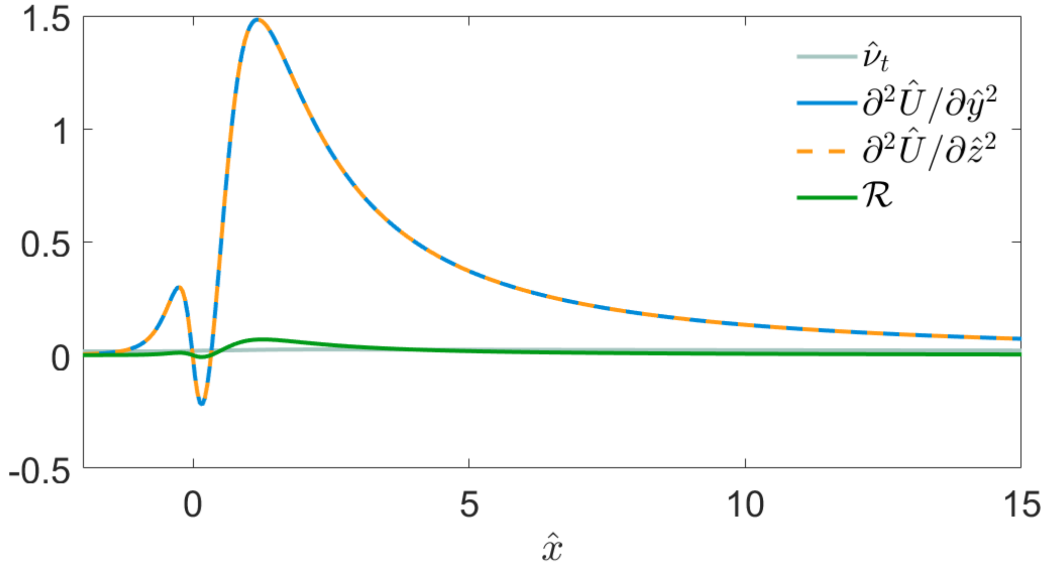

Figure 1: An example of streamwise variation of the centreline $\mathcal{R}$ and its component.

- Major comment 3: Equation 23 is incorrect

  We thank the referee for pointing this out. The implicit function theorem was not applied correctly in our original manuscript. We replace the derivation from equations 21 to 23 with the following analysis, which leads to the same result. This derivation process is included as an appendix.

  From the equation of interest

$$\mathcal{R}_3 = \int_{-\infty}^{\hat{x}_3} \mathcal{R} d\xi, \tag{1}$$

  we take the derivative with respect to $\hat{x}_3$ to study how this intersection point changes with turbulence level (i.e. $\hat{x}_3$ is a function of the inflow turbulence intensity), which gives

$$\frac{\partial \mathcal{R}_3}{\partial \hat{x}_3} = \frac{\partial \int_{-\infty}^{\hat{x}_3} \mathcal{R} d\xi}{\partial \hat{x}_3}. \tag{2}$$

  We keep the left-hand side of the equation in its current form, and attempt to find what $\frac{\partial \int_{-\infty}^{\hat{x}_3} \mathcal{R} d\xi}{\partial \hat{x}_3}$ is. Note that $\frac{\partial \int_{-\infty}^{\hat{x}_3} \mathcal{R} d\xi}{\partial \hat{x}_3}$ is not the same as $\frac{\partial \int_{-\infty}^{\hat{x}_3} \mathcal{R} d\xi}{\partial \hat{x}}$. We model $\frac{\partial \int_{-\infty}^{\hat{x}_3} \mathcal{R} d\xi}{\partial \hat{x}_3}$ by the following process.

We assume $\mathcal{R}(\hat{x})$ is a self-similar function over different inflow turbulence intensities, such that

$$\frac{\mathcal{R}}{R_{max}} = f(\frac{x}{\eta}), \tag{3}$$

where $\mathcal{R}_{max}$ is the maximum value of $\mathcal{R}$, and η is a length scale, which we take as the $\hat{x}$ value at which $\mathcal{R}_{max}$ occurs. When the inflow turbulence intensity increases by a small amount ΔTi, $\mathcal{R}$ becomes

$$\mathcal{R}^* = (1+\epsilon)\mathcal{R}_{max} f(\frac{\hat{x}}{\eta/(1+\epsilon)}), \tag{4}$$

where ϵ is a small quantity induced by the change in the inflow turbulence intensity. This means the profile of $\mathcal{R}$ (plotted against $\hat{x}$, see Fig 3 below) is stretched along the y-axis by $(1+\epsilon)$, and compressed along the x-axis by $(1+\epsilon)$, so that the area under the curve remains the same, which corresponds to energy conservation along the wake centreline, as implied by Eq. (24) in the modified manuscript. Thus, we obtain

$$\mathcal{R}^*(\hat{x}) = (1+\epsilon)\mathcal{R}((1+\epsilon)\hat{x}) \tag{5}$$

Meanwhile, for the same small increase in the inflow turbulence, $I(x) = \int_{-\infty}^{\hat{x}} \mathcal{R} d\xi$ becomes

$$I^*(\hat{x}) = \int_{-\infty}^{\hat{x}} \mathcal{R}^*(\hat{x})d\hat{x} = \int_{-\infty}^{(1+\epsilon)\hat{x}} (1+\epsilon)\mathcal{R}(\hat{x}(1+\epsilon))\frac{d\hat{x}(1+\epsilon)}{(1+\epsilon)} = \int_{-\infty}^{(1+\epsilon)\hat{x}} \mathcal{R}((1+\epsilon)\hat{x})d(1+\epsilon)\hat{x} = I((1+\epsilon)\hat{x}), \tag{6}$$

which means the profile of I (plotted against $\hat{x}$) is compressed along the x-axis by $(1+\epsilon)$ to get I^* for a small increase in the inflow turbulence. This means for the point where $I^*(\hat{x}_3^{'}) = \mathcal{R}_3$ is satisfied, where $\hat{x}_3^{'} = \hat{x}_3/(1+\epsilon)$, the change in the $\hat{x}$ position is $\Delta\hat{x} = \hat{x}_3 - \hat{x}_3/(1+\epsilon)$, see Fig. 3 below. At $\hat{x}_3^{'}$, $\mathcal{R}$ increases by $\Delta\mathcal{R} = \mathcal{R}^*(\hat{x}_3^{'}) - \mathcal{R}(\hat{x}_3) = (1+\epsilon)\mathcal{R}(\hat{x}_3) - \mathcal{R}(\hat{x}_3) = \epsilon\mathcal{R}_3$. Since $\epsilon \ll 1$, we assume $\Delta\hat{x} = \epsilon\hat{x}_3/(1+\epsilon) = \epsilon\hat{x}_3$. Thus,

$$\frac{\Delta\mathcal{R}}{\Delta\hat{x}} = \frac{\mathcal{R}_3}{\hat{x}_3}. \tag{7}$$

Meanwhile, the new intersection point occurs at $(\hat{x}_3^*, \mathcal{R}_3^*)$, where $\hat{x}_3^* = \hat{x}_3 - \Delta\hat{x}_3$ and $\mathcal{R}_3^* = \mathcal{R}_3 + \Delta\mathcal{R}_3$. Note that $-\Delta\mathcal{R}_3/\Delta\hat{x}_3$ represents $\partial\int_{-\infty}^{\hat{x}_3} \mathcal{R}d\xi/\partial\hat{x}_3$ that we want to find.

To find $\Delta\mathcal{R}_3/\Delta\hat{x}_3$, we first find $\Delta\mathcal{R}/\Delta\hat{x}$. As shown in Eq. (7), $\Delta\mathcal{R}/\Delta\hat{x}$ is equal to $\mathcal{R}_3/\hat{x}_3$, which requires more information on the profile of $\mathcal{R}$. For unblocked flow, the wake centreline velocity is governed by

$$\alpha\frac{\partial\alpha}{\partial\hat{x}} = \mathcal{R} \tag{8}$$

in the far wake. We integrate this equation along the streamwise direction from the point of interest to far downstream where the wake recovers, which gives

$$\frac{1}{2}(1-\alpha^2) = \frac{C_t}{2} - I \tag{9}$$

Then, we can express $I/\mathcal{R}$ in terms of α. Because the centreline velocity recovers by receiving energy from the spanwise direction, we can assume the centreline velocity varies relatively slowly in the streamwise direction, so that its derivatives with respect to the streamwise direction decrease with increasing order, and we can show that the third derivative and other higher-order derivatives of $I/\mathcal{R}$ are negligible. Since the first two derivatives of $I/\mathcal{R}$ are not negligible, we can approximate $I/\mathcal{R}$ by a second-order polynomial function of $\hat{x}$, so we have

$$\left(\frac{I}{\mathcal{R}}\right) = a\hat{x}^2 + b\hat{x} + c, \tag{10}$$

where a, b and c are coefficients of the polynomials. At $\hat{x} = 0$, $I = 0$ and $\partial I/\partial\hat{x} = \mathcal{R} = 0$, which suggests

$$\frac{I}{\mathcal{R}} = a\hat{x}^2 + b\hat{x}, \tag{11}$$

where $b\hat{x} \ll a\hat{x}^2$, as is implied by the RANS results in Fig. 2 below. From Eq. (11), we can calculate the value of $\mathcal{R}_3/\hat{x}_3$.

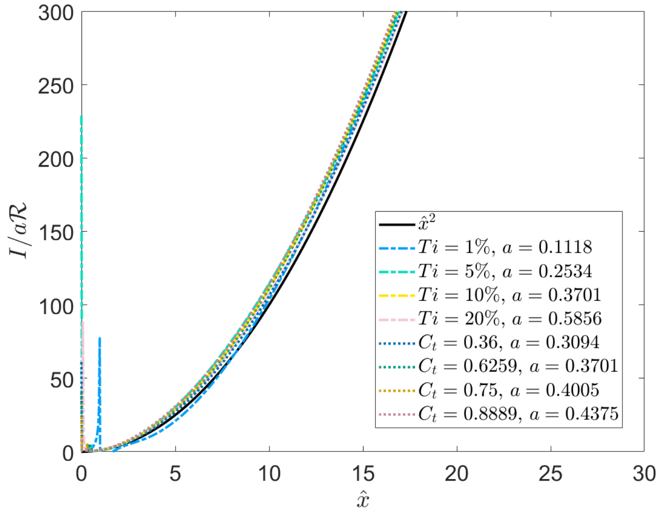

Figure 2: The fitting of simulation results, $I/\mathcal{R}$, to $a\hat{x}^2$ for a range of thrust coefficients and inflow turbulence intensities.

At $\hat{x}_3$, we have $I = R$, so

$$a\hat{x}_3^2 + b\hat{x}_3 = 1. \tag{12}$$

Meanwhile,

$$\frac{\partial}{\partial \hat{x}}\left(\frac{I}{\mathcal{R}}\right) = 1 - \frac{I\partial\mathcal{R}/\partial\hat{x}}{\mathcal{R}^2} = 2a\hat{x} + b, \tag{13}$$

so at $\hat{x}_3$,

$$1 - \frac{(\partial\mathcal{R}/\partial\hat{x})_3}{\mathcal{R}_3} = 2a\hat{x}_3 + b. \tag{14}$$

Equation (12) can be rearranged to

$$\frac{1}{\hat{x}_3} = \frac{1}{2}(2a\hat{x}_3 + b + b). \tag{15}$$

Since $b \ll a\hat{x}_3$ as we previously assumed, there is

$$\frac{1}{\hat{x}_3} - \frac{2a\hat{x}_3 + b}{2} \ll \frac{1}{2}\frac{2a\hat{x}_3 + 2b}{2}. \tag{16}$$

We then use Eq. (14) to replace $2a\hat{x}_3 + b$, which gives

$$\frac{1}{\hat{x}_3} - \frac{1 - (\partial\mathcal{R}/\partial\hat{x})_3/\mathcal{R}_3}{2} \ll \frac{1}{2}\frac{1}{\hat{x}_3}. \tag{17}$$

As shown in Fig. 3 below, we define $\Delta\hat{x}_{\mathcal{R}} = \Delta\hat{x} - \Delta\hat{x}_3$, and there is also

$$\Delta\hat{x}_{\mathcal{R}} = \frac{\Delta\mathcal{R}}{\mathcal{R}_3 - (\partial\mathcal{R}/\partial\hat{x})_3} = \frac{\mathcal{R}_3}{\hat{x}_3}\frac{\Delta\hat{x}}{\mathcal{R}_3 - (\partial\mathcal{R}/\partial\hat{x})_3}. \tag{18}$$

We multiply Eq. (17) with $\frac{\mathcal{R}_3\Delta\hat{x}}{\mathcal{R}_3 - (\partial\mathcal{R}/\partial\hat{x})_3}$, which gives

$$\Delta\hat{x}_{\mathcal{R}} - \frac{1}{2}\Delta\hat{x} \ll \frac{1}{2}\Delta\hat{x}_{\mathcal{R}}. \tag{19}$$

Recall that $\Delta\hat{x}_3 = \Delta\hat{x} - \Delta\hat{x}_{\mathcal{R}}$, so there is

$$\Delta\hat{x}_{\mathcal{R}} - \Delta\hat{x}_3 = 2\Delta\hat{x}_{\mathcal{R}} - \Delta\hat{x} \ll \Delta\hat{x}_{\mathcal{R}} \tag{20}$$

Thus,

$$\frac{\Delta\mathcal{R}_3}{\Delta\hat{x}_3} - \frac{\Delta\mathcal{R}_3}{\Delta\hat{x}_{\mathcal{R}}} \ll \frac{\Delta\mathcal{R}_3}{\Delta\hat{x}_3}. \tag{21}$$

As ΔTi tends to zero, $\frac{\Delta\mathcal{R}_3}{\Delta\hat{x}_{\mathcal{R}}}$ tends to $\mathcal{R}_3$, and $\frac{\Delta\mathcal{R}_3}{\Delta\hat{x}_3}$ tends to $-\frac{\partial\int_{-\infty}^{\hat{x}_3}\mathcal{R}d\xi}{\partial\hat{x}_3}$, so there is

$$\mathcal{R}_3 + \frac{\partial\int_{-\infty}^{\hat{x}_3}\mathcal{R}d\xi}{\partial\hat{x}_3} \ll -\frac{\partial\int_{-\infty}^{\hat{x}_3}\mathcal{R}d\xi}{\partial\hat{x}_3}. \tag{22}$$

Recall that

$$\frac{\partial\mathcal{R}_3}{\partial\hat{x}_3} = \frac{\partial\int_{-\infty}^{\hat{x}_3}\mathcal{R}d\xi}{\partial\hat{x}_3} = \frac{\partial\int_{-\infty}^{\hat{x}_3}\mathcal{R}d\xi}{\partial\hat{x}_3} + \mathcal{R}_3 - \mathcal{R}_3. \tag{23}$$

Since $\frac{\partial\int_{-\infty}^{\hat{x}_3}\mathcal{R}d\xi}{\partial\hat{x}_3} + \mathcal{R}_3$ is negligible compared to $-\frac{\partial\int_{-\infty}^{\hat{x}_3}\mathcal{R}d\xi}{\partial\hat{x}_3}$, we can approximate $\partial\mathcal{R}_3/\partial\hat{x}_3$ as

$$\frac{\partial\mathcal{R}_3}{\partial\hat{x}_3} \approx -\mathcal{R}_3 \tag{24}$$

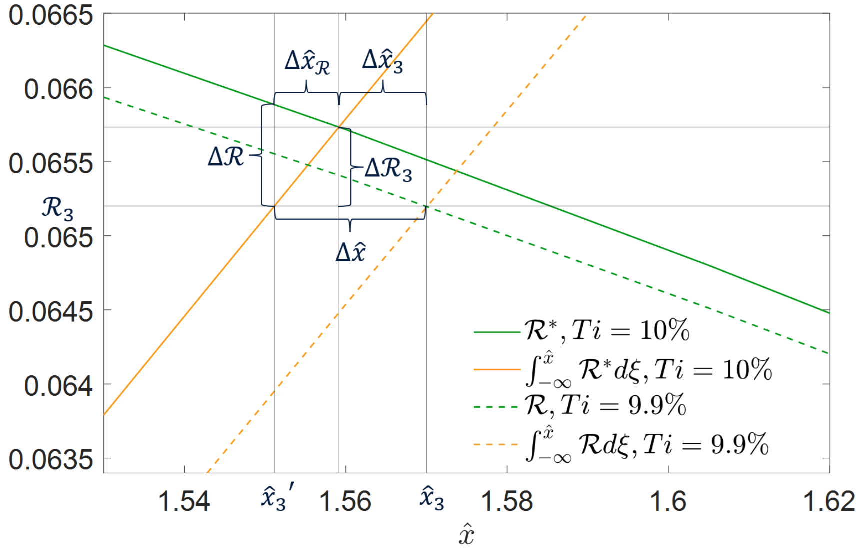

Figure 3: The change in the intersection point due to a small change in inflow turbulence intensity.

- Major comment 4: Equation 24 and the constant of integration

  We thank the referee for pointing out this important issue. We agree that the original text did not sufficiently distinguish between the mathematical definition of $\hat{x}_3$ and its physical interpretation as the transition point to the far wake.

  In the original manuscript, $\hat{x}_3$ was introduced through the condition, $\mathcal{R}_3 = \int_{-\infty}^{\hat{x}_3}\mathcal{R}(\xi)d\xi$. As the referee correctly notes, when $\hat{\nu}_t = 0$, we have $\mathcal{R} = 0$ by definition. The above condition then degenerates into the identity, 0=0, and therefore no longer selects a unique value of $\hat{x}_3$. Thus, the statement that $\hat{x}_3$ can be determined directly from this condition in the limiting case $\hat{\nu}_t = 0$ is not mathematically rigorous. We have revised the manuscript to avoid this implication.

  The corrected interpretation is as follows. The limiting cases $\hat{\nu}_t \to 0$ and $\hat{\nu}_t \to \infty$ should not be taken as exact cases in which the defining equation remains well posed. Instead, they are used as asymptotic modelling constraints for estimating the integration constant in Eq. 24. In the limit $\hat{\nu}_t \to 0$, turbulent mixing vanishes, the Reynolds-stress divergence term satisfies $\lim_{\hat{\nu}_t \to 0} \mathcal{R} = 0$, and the physical interpretation is that the wake does not recover through turbulent diffusion. Therefore, the far-wake onset is pushed progressively downstream, which we express as $\lim_{\hat{\nu}t \to 0} \hat{x}_3 = \infty$.

This statement is not derived from the mathematical condition $\mathcal{R} = \int \mathcal{R} d\xi$ at $\hat{\nu}_t = 0$. Rather, it is an asymptotic physical constraint introduced to close the model.

Similarly, the limiting case $\hat{\nu}_t \to \infty$ should be interpreted as an idealised asymptotic condition rather than an attainable physical state. As the turbulence level increases, wake recovery becomes more rapid, and the region over which $\mathcal{R}$ is non-zero becomes increasingly concentrated near the actuator disc. Consequently, the transition location $\hat{x}_3$ is expected to move upstream towards its minimum admissible value, namely the disc location $\hat{x}_2$: $\lim_{\hat{\nu}t \to \infty} \hat{x}_3 = \hat{x}_2$.

At the same time, the accumulated contribution of $\mathcal{R}$ up to $\hat{x}_3$ approaches the total streamwise contribution of $\mathcal{R}$, which is $\int_{-\infty}^{\infty} \mathcal{R}(\xi) d\xi$. This expression should not be read as evaluating $\mathcal{R}$ exactly at $\hat{x} = 0$, nor as imposing $\mathcal{R}(0) = \int_{-\infty}^{\infty} \mathcal{R}(\xi) d\xi$. Instead, it represents the asymptotic limit in which the non-zero values of $\mathcal{R}$ become increasingly concentrated around the disc location $\hat{x}_2$. In this idealised limit, $\mathcal{R}$ behaves formally like a highly localized distribution. The total integrated contribution remains finite, while the streamwise region over which it acts becomes vanishingly small. We have revised the manuscript to make it clear that this is a modelling idealisation used to infer the limiting behaviour of the proposed relation, not a physical description of the velocity or turbulence field.

We also agree with the referee that the turbine location should be denoted consistently as $\hat{x} = \hat{x}_2$, rather than $\hat{x} = 0$. This notation has been clarified in the revised manuscript.

Regarding the statement that the wake is fully recovered at the disc position, we agree that the previous wording was misleading. The intended argument was not that the physical wake becomes instantaneously recovered at the disc. Rather, in the idealised limit of infinitely strong turbulent mixing, the velocity deficit would be removed over an infinitesimally short downstream distance. Hence, the normalised centreline velocity approaches $\alpha \to 1$ immediately downstream of the disc in this asymptotic case. We have revised the text to state this more carefully.

In summary, we have revised the manuscript in Section 3.3 from line 252 to 256 to clarify that the limiting cases used in determining the integration constant are not obtained by directly substituting $\hat{\nu}_t = 0$ or $\hat{\nu}_t = \infty$ into the mathematical definition of $\hat{x}_3$. Rather, they are asymptotic physical constraints used to close the model. We have also clarified the notation for the turbine location and the interpretation of the large $\hat{\nu}_t$ limit.

- Major comment 5: Momentum conservation condition

  We thank the referee for identifying this ambiguity. We agree that Section 3.6 did not clearly explain the connection between the discussion of the Gaussian wake profile and the subsequent modification of the momentum-conservation condition. We have revised this section to make the mathematical and physical basis of the correction more explicit.

  First, we clarify that the modification introduced in Section 3.6 is not part of the definition of $\hat{x}_3$, nor is it applied only at the start of the far wake. The location $\hat{x}_3$ is defined independently through the condition discussed earlier in the manuscript. Section 3.6 addresses a separate issue: how should the amplitude and width of a Gaussian profile be constrained by the momentum balance in the presence of the blockage effect?

  The exact global momentum balance applies to the full velocity and pressure fields. In nondimensional form, the unmodified expression is

$$\int_{A_c} \hat{U}(1 - \hat{U}) dA - \frac{1}{2}(\beta^2 - 1) A_c = T/\rho U_\infty^2, \tag{25}$$

  where the second term represents the pressure contribution approximated using the Bernoulli equation. This expression is appropriate only if the assumed velocity and pressure fields capture the relevant cross-sectional contributions to the global momentum balance.

  The difficulty is that the Gaussian wake profile is an approximated representation of the wake core. It does not represent the weak but spatially extended velocity increase outside the wake (i.e. bypass flow acceleration) that is crucial to the global mass conservation, nor does it fully represent the corresponding pressure perturbation over the whole cross-section. In an unblocked or weakly blocked flow, these outer-region differences are small in magnitude and are often neglected, but their area integrals are considerable. In that case, the commonly used relation

$$\int_{A_c} \hat{U}(1-\hat{U})dA = T/\rho U_\infty^2, \tag{26}$$

should be interpreted as momentum balance over the wake region rather than the entire cross-sectional domain.

In a blocked flow, the same issue remains, which means the Gaussian profile should not be applied to the global momentum balance. Directly substituting a Gaussian wake profile into the unmodified global momentum equation forces the Gaussian profile to compensate for flow features that it does not represent, and produces a poor prediction near the wake centre, which is the main output of the wake model. Meanwhile, the bypass acceleration outside the wake is no longer negligible in magnitude, and neither is the pressure drop. Thus, it is difficult to estimate the momentum deficit within the wake region directly.

We thus introduce the correction by comparing the blocked case with a corresponding hypothetical unblocked reference case. The purpose of this reference case is to isolate the change in pressure and bypass-flow contribution associated with blockage. This leads to the modified closure

$$\int_{A_c} \hat{U}(1-\hat{U})dA - \frac{1}{2}(\beta-1)(\beta+2\alpha-1)A_c = \frac{T}{\rho U_\infty^2}. \tag{27}$$

The correction term $\frac{1}{2}(\beta-1)(\beta+2\alpha-1)A_c$ is introduced to estimate the portion of the pressure contribution due to blockage, and cancels out the momentum increase in $\int_{A_c} \hat{U}(1-\hat{U})dA$ captured by the Gaussian profile, so that the modified momentum equation (Eq. (23) in the letter) describes the momentum deficit within the wake.

However, as the blockage ratio and the inflow turbulence intensity increase, the area integral of the discrepancy between the Gaussian profile and the actual wake profile reduces, and the solution tends to the unmodified solution. Thus, we take the average of the two expressions to obtain a more robust solution, given as

$$\int_{A_c} \hat{U}(1-\hat{U})dA - \frac{1}{2}(\beta-1)(\beta+\alpha)A_c = \frac{T}{\rho U_\infty^2} \tag{28}$$

We also clarify in the revised manuscript that this correction is a semi-empirical closure rather than an exact derivation from the global momentum equation. Its role is to estimate the momentum deficit within the wake under blockage. The RANS results are used not as the sole justification for the modification, but as evidence that the unmodified closure with Gaussian profile leads to systematic errors in the predicted global momentum deficit.

Finally, we have revised the text in Section 3.6 so that the logical connection is explicit. The revised argument is now:

- (i) the Gaussian profile approximates the wake core but does not represent the full cross-sectional velocity and pressure fields;
- (ii) in either blocked or unblocked flows, the omitted outer-flow and pressure contributions have a non-negligible area-integrated effect;
- (iii) therefore, using the unmodified global momentum condition with a Gaussian profile introduces a systematic error;
- (iv) the modified momentum condition is introduced as a correction for this unresolved contribution.

We have also revised the wording to avoid implying that the correction is derived solely from the observation that the Gaussian profile overestimates or underestimates the velocity deficit near the wake boundary. That observation is now presented only as supporting evidence of the limitations of the Gaussian approximation, while the correction itself is motivated by the need to account for the missing area-integrated contribution of the outer flow and pressure field.

- Minor comments:
  - Inclusion of marching approach for literature review:
    Several major type of marching methods are included in the introduction from line 29 to 34 are included in the revised manuscript.
  - Yellow curve in Fig. 2: The yellow curve almost coincides with the purple curve, which is why it is not visible. The purple curve is now changed to a dashed line, so that the yellow is visible.
  - Caption in Fig 2:
    The velocity gradient is not used for the mesh convergence study, and the caption of Fig. 2 is now corrected.
  - Eq. 17 is a momentum equation instead of an energy equation:
    Although Eq. 17 is derived from the streamwise component of RANS equation as shown in the manuscript, it describes the energy flux balance within the centreline streamtube, similar to the Bernoulli equation. The clarification is included right behind Eq. 17 in line 195 in the revised manuscript.
  - Illustration of the procedure:
    Since the detailed procedure will be described in section 3.7, the same process is not repeated at the end of section 3.4. The reader is referred to the section where the procedure is described in line 289 and line 290.
  - regarding 'simplified momentum equation':
    This whole section (section 3.6) is now rewritten.
  - Location at which the wake profile is taken in Figure 5:
    The location at which the velocity profile is taken is now stated in the figure caption.
  - regarding line 425:
    The wording for that sentence is changed. The sentence is now in line 510 in the revised manuscript.

Response to reviewer 2

- Major comment 1: Derivation of the transition criterion, Eqs. (22)-(28)

  From equations 22 to 23, a new derivation process is now included in the Appendix of the revised manuscript. It is based on the assumption that the divergence of the Reynolds shear stresses along the wake centreline is a self-similar function for different turbulence intensities, and that the streamwise derivatives of the wake centreline velocity decrease with order so that $\int_{-\infty}^{\hat{x}} \mathcal{R} d\xi$ can be approximated by a second-order polynomial.

  From equations 23 to 24, we adopt an asymptotic solution for the constant of integration. It is based on the observation that as inflow turbulence increases, $\hat{x}_3$ decreases and $\mathcal{R}_3$ increases. Thus, as the inflow turbulence increases to become extremely large, the wake recovers over a negligibly small distance, so that $\hat{x}_3$ tends to the disc position and $\mathcal{R}_3$ also tends to its maximum value, $\int_{-\infty}^{\infty} \mathcal{R} d\hat{x}$.

  From equations 25 to 27, we calculate the value of $\int_{-\infty}^{\infty} \mathcal{R} d\hat{x}$. When the wake fully recovers, the velocity returns to the freestream level, and $\int_{-\infty}^{\infty} \mathcal{R} d\hat{x}$ describes the total energy per unit mass flux transferred to the wake centreline to achieve this recovery, which is determined by the pressure difference in the relevant sections.

  Equation 28 is a rearrangement of equation 27.

- Major comment 2: Modified momentum expression introduced in Section 3.6

  The change in the momentum equation should be viewed as a pragmatic modification. The reason we need this modification is because the Gaussian profile does not capture the velocity profile accurately especially outside the wake core. From mass conservation, we know there must a region outside the wake where the velocity is larger than the freestream velocity. When we use the momentum equation

$$\int_{A_c} \hat{U}(1-\hat{U}) dA - \frac{1}{2}(\beta^2 - 1) A_c = T/\rho U_\infty^2 \tag{29}$$

to calculate the global momentum deficit, the momentum flux calculated by the Gaussian-profiled velocity field is underestimated. Thus, for the unblocked flow, the above equation combined with the Gaussian profile is not a good representation of global momentum conservation, but is a good representation of local momentum conservation within the wake region.

For the blocked flow, the Gaussian profile still underestimates the momentum flux in the bypass region, and does not give accurate global momentum deficit. Thus, we attempt to calculate the local momentum deficit by making reference to the unblocked flow, which produces the modified equation,

$$\int_{A_c} \hat{U}(1-\hat{U})dA - \frac{1}{2}(\beta-1)(\beta+2\alpha-1)A_c = T/\rho U_\infty^2. \tag{30}$$

However, as the blockage ratio and the inflow turbulence intensity increases, the value of the underestimated momentum flux reduces, which turns the solution to the unmodified momentum equation. Thus, we take the average of the two equations for a more robust solution, which is

$$\int_{A_c} \hat{U}(1-\hat{U})dA - \frac{1}{2}(\beta-1)(\beta+\alpha)A_c = T/\rho U_\infty^2. \tag{31}$$

We have revised Section 3.6 so that the motivation and the physical basis for this modification are clear.

- Major comment 3: Validation and interpretation of the proposed transition location

  The quantitative analysis of the accuracy of $\hat{x}_3$ is now added to the result section from line 395 to 425, and the detailed data for the error analysis are shown in Table 3, 4 and 5. The discussion of the relevance of the behaviour of the proposed model with existing near-wake length models is also added in line 266 to 271.

- Major comment 4: Dependence on the turbulence closure

  Although the concept of the eddy viscosity hypothesis was introduced very early in the derivation process in our original manuscript, it is not required for the near-wake length model proposed. Thus, any reasonable closure for the Reynolds shear stresses can be chosen. The eddy viscosity hypothesis is now introduced later in the revised manuscript in Section 3.5 from line 292 to 299 so that this is clear.

- Minor comments:

  - Naming of the cases:

    In the revised manuscript, we name each case by its flow condition characteristics instead of numbers. Table 1 is now modified such that this is clear.

  - Caption of Figure 2:

    The velocity gradient is not used for the mesh convergence study. The Caption of Figure 2 is now corrected.

  - The schematic representation of Stage 4 in Figure 3:

    Stage 4 in Figure 3 is now represented by swirls in the shaded area. Clarification is also included in the figure caption.

  - Middle expression in Eq. 28:

    Eq. 28 in the original manuscript is now Eq. 26 in the revised manuscript. The middle expression is removed and introduced later, where this expression is derived from lines 292 to 299 in the revised manuscript.

Response to reviewer 3

- Major comment 1: Inconsistency regarding the physical definition of the near wake distance

  We thank the referee for pointing out the inconsistency in the definition. We admit the concepts could have been explained more clearly. In our revised manuscript, we clarify that the point where the pressure gradient is negligible is not used as a definition of the transition to far wake. Rather, the start of the far wake is defined as the inflection point of the wake centreline velocity α. However, since the dominant driving forces of the variation of the wake centreline velocity are $\partial\hat{p}/\partial\hat{x}$ and $\mathcal{R}$ as shown in Section 3.1, we take the start of the far wake to be at the location where $\mathcal{R} - \partial\hat{p}/\partial\hat{x}$ reaches its maximum. Once $\mathcal{R} - \partial\hat{p}/\partial\hat{x}$ reaches its maximum, the velocity profile is assumed to be fully developed and reaches a self-similar state. When $\mathcal{R} - \partial\hat{p}/\partial\hat{x}$ is maximum, $\partial\hat{p}/\partial\hat{x}$ should also be negligible compared with $\mathcal{R}$. How the proposed definition of the start of the far wake is related to the location beyond which the velocity profile becomes self-similar is explained as follows. In this case, as is adopted by many studies, we take the self-similar velocity profile to be Gaussian.

The evolution of the wake profile is directly linked to the streamwise variation of the Reynolds-stress divergence, $\mathcal{R}$. Two distinct regimes can be identified.

In the first regime, the wake profile evolves from the initial state, which is usually taken to be top-hat, to the self-similar state, which is usually taken to be Gaussian. During this stage, the profile evolution itself contributes to an increase in $\mathcal{R}$. In the second regime, once the profile has become self-similar, the subsequent evolution of $\mathcal{R}$ is governed primarily by changes in the maximum velocity deficit, C, and wake width, σ. Importantly, here $\mathcal{R}$ decreases with the reduction of C and the increase of σ. Thus, the wake profile tends to be self-similar (Gaussian) in the region where $\mathcal{R}$ decreases.

Since $\partial\hat{p}/\partial\hat{x}$ continuously decreases downstream of the turbine towards the far wake, the maximum $\mathcal{R} - \partial\hat{p}/\partial\hat{x}$ occurs downstream of the maximum $\mathcal{R}$. This means that the wake profile tends to be already self-similar where $\mathcal{R} - \partial\hat{p}/\partial\hat{x}$ is maximum.

It should be noted that a limiting case may exist under very low inflow turbulence in which the wake profile has not fully developed when $\mathcal{R}$ begins to decrease. However, in such a situation, the profile must already be close to the fully developed state. Otherwise, the continuing profile-shape evolution would still provide a considerable positive contribution to $\mathcal{R}$, preventing the observed net decrease.

This explanation is included from line 215 to line 226 and line 234 in the revised manuscript.

- Major comment 2: The location of maximum $\mathcal{R} - d\hat{p}/d\hat{x}$ approximately coincides with the location where the streamwise integral of $\mathcal{R}$ is equal to $\mathcal{R}$

  We thank the referee for the comment. We agree that this is a crucial point of the proposed model. We have included the explanation on why these two points are close in lines 232 and 234. Essentially, the point where $\mathcal{R} = \int_{-\infty}^{\hat{x}} \mathcal{R} d\xi$ and the maximum $\mathcal{R} - \partial\hat{p}/\partial\hat{x}$ are close because $\mathcal{R} = \int_{-\infty}^{\hat{x}} \mathcal{R} d\xi$ is observed to occur at large $\mathcal{R}$ and small $\partial\hat{p}/\partial\hat{x}$, and the maximum $\mathcal{R} - \partial\hat{p}/\partial\hat{x}$ should occur when $\partial\hat{p}/\partial\hat{x}$ is small compared to $\mathcal{R}$ by physical reasoning. Based on this shared tendency, we assume these two points are close, and this assumption is independent of the turbulence model.

  We revised the manuscript such that the eddy viscosity hypothesis is introduced later in the text. Both the proposed condition, $\mathcal{R} = \int_{-\infty}^{\hat{x}} \mathcal{R} d\xi$, and the constant of the integral for the proposed near-wake length model are independent of the turbulence model. This has been made clear in the revised manuscript, as shown from line 166 to line 176 in Section 3.1, and line 257 to line 265 in Section 3.3. The eddy viscosity hypothesis is used as a modelling choice for $\mathcal{R}$ and does not affect the model formulation. We also included Tables 3 to 5 to quantitatively assess how close these two points are.

- Major comment 3: Inconsistency in the application of the boundary condition of equation 24

  We have revised the explanation of how the boundary condition is chosen in Section 3.3 from line 252 to line 256. The condition at extremely high turbulence is used to close the model as an asymptotic case. As the turbulence level increases, the near-wake position $\hat{x}_3$ moves closer to the disc position and the corresponding divergence of the Reynolds shear stresses $\mathcal{R}_3$ increases. Thus, under extremely high turbulence level, $\hat{x}_3$ tends to the disc position, and $\mathcal{R}_3$ tends to its maximum possible value $\int_{-\infty}^{\infty} \mathcal{R} d\xi$. Although this condition is used to get the constant of the integration, we do not intend to use the model for such high turbulence scenarios since it falls out of the parameter space for wind turbine application.

  Additionally, for the derivation of the constant of integration, the eddy viscosity hypothesis is not required. This constant is a result of energy conservation, as shown from line 257 to line 260.

  In terms of whether the intersection point of $\mathcal{R} = \int_{-\infty}^{\hat{x}} \mathcal{R} d\xi$ captures the defined start of the far wake for extremely high turbulence condition, this does not affect the performance of the model because $\mathcal{R} =$

$\int_{-\infty}^{\hat{x}} \mathcal{R} d\xi$ is a point that will always occur in the wake. Thus, the predicted $\hat{x}_3$ and $\mathcal{R}_3$ should always predict a point in the wake. This point may be upstream or downstream of the defined transition point, but it is less important in a practical sense.

- Minor comment: Literature review of wake models considering the near-wake behaviour:

  Several wake models that consider the near-wake transition as well as the role of pressure gradient are included in the introduction section from line 35 to 41.